# Tunnel-boring in soft soil: a study on the driving forces applied to a slurry-shield TBM

Daniele Festa[1], Wout Broere[1], Johan W. Bosch[1]

[1]TU Delft, Civil Engineering Dept., The Netherlands

## ABSTRACT

The use of Tunnel Boring Machines (TBMs) in difficult ground conditions and built-up areas has proven to be an effective and safe construction method. Even so, the state-of-the-art technology still involves a trial-and-error approach. This seems mainly due to an incomplete understanding of the physics governing the interaction between the TBM and the surrounding soil. Due to such uncertainty, the predictions of soil settlements induced by the construction of a tunnel are often unreliable. Studying the TBM's behaviour, on one side, and the soil response, on the other, can contribute to a better understanding of the TBM-soil interaction. This paper quantifies the driving forces applied to a slurry-shield TBM in sand, together with their spatial and temporal distribution. To this end, the monitoring-data of the Hubertus Tunnel in The Hague, The Netherlands, was processed. Results show the 'missing link' to equilibrate the system of forces and moments acting on the TBM. This 'missing link' is supplied by the soil reaction on the TBM, and is validated by the kinematic behaviour of the TBM. This also demonstrates the value of the TBM logged data with respect to fundamental scientific research on bored tunnels.

## 1 INTRODUCTION

Tunnel Boring Machines (TBMs) are more and more used to construct tunnels in challenging environments, such as built-up areas. As a construction technique, it has widely proven to be effective and socially acceptable. Nevertheless, municipalities are setting increasingly stricter standards on design engineers, TBM manufacturers and operators. Therefore, predictive risk analyses come into play, as most of the political and technical decisions are based on these. In particular in the design stage, risk analyses are used to predict how the tunnel construction will affect its surroundings. However, predictions are still largely based on the experience gained from previous projects, therefore often lacking in adequate case-specificity. In other words, the expected level of risk is defined through worst scenario figures, usually expressed in terms of a 'volume loss' rate obtained from the records of previous tunnels bored in similar circumstances. The 'volume loss' is then processed via empirical, analytical, or numerical analyses, such as to derive the expected absolute and differential settlements of the surrounding soil and constructions. Finally, based on criteria of acceptable damage, it is judged whether the project is technically feasible and socially acceptable. However, according to this 'conventional' approach, settlement predictions are hardly correlated with project-specific features, such as the TBM's specifications and its real kinematic behaviour when driven through the soil. Consequently, the predictions' accuracy and their reliability risk to be negatively affected. In this context, the interaction processes between the TBM, the soil, and the process fluids certainly represent a critical aspect. Their better understanding can lead to an improvement with respect to the reliability of the overall tunnel boring process.

The disregard of TBM features and operation is surprising, particularly considering that observed longitudinal settlement profiles show the remarkable effect of the TBM-shield transit on the overall induced surface settlements, as also shown by the interaction model between the TBM-shield and the surrounding soil by Kasper and Meschke (2006). However, their model approaches the tunnel-construction problem theoretically, aiming to find

adequate validation from real cases at a later stage. In this research an opposite approach is proposed, namely to investigate the system of forces and pressures actually applied to drive a slurry-shield TBM. The study is based on the monitoring-data collected during the construction of the Hubertus Tunnel, a double-tube road tunnel located in The Hague, The Netherlands. The tunnel, excavated in 2006 and 2007, was selected for two reasons: first, the combined availability of TBM and soil-displacement monitoring data, and second, given its recent completion, the accurate feedback likely to be obtained from people involved in the project.

Even if the practice of controlling the TBM driving parameters is well established for construction purposes, this research tries to mine the complete series of recorded data, and investigates how this can contribute to an improved understanding of the interaction between the TBM and the surrounding soil. The analyses and results presented here are the second step of a wider research effort aimed to clarify the TBM-soil interaction problem. The first step has quantified the interface-displacements between the excavated soil profile and the shield-body, which was obtained by a kinematical analysis of the TBM-shield behaviour (see Festa et al. (2011 a, b)). In the upcoming stage, the displacements-field derived at step one will be transformed into a stress-distribution at the shield-soil interface. Finally, in the fourth stage, the equilibrium between the applied forces and pressures (active system) and the soil reaction (passive system) will be determined.

## 2 THE DATA ANALYSIS

### *2.1 The Hubertus tunnel*

The Hubertus tunnel consists of two parallel tubes, north and south, 1666.70 m and 1653.48 m long, respectively. The tubes were excavated by a non-articulated 10 680 mm long Herrenknecht slurry-shield type TBM, with a front diameter of 10 510 mm, and a rear one of 10 490 mm (i.e. with a radial tapering of 10 mm). A standard radial overcutting of 10 mm was permanently used. The cutting wheel was supported by a longitudinally displaceable spherical bearing, and handled via three couples of hydraulic cylinders. The tail-void grouting occurred via the upper four of the six injection openings distributed along the shield tail. The final lining is formed by 2 m long prefab reinforced-concrete elements, with an external diameter of 10 200 mm. The theoretical tail-void gap is 165 mm. The sharpest horizontal curve, with a curvature radius of 542.3 m, is located in the south alignment, and was bored in leftward direction. The deepest point of the tunnel axis is located at 27.73 m below surface. Further details concerning the tunnel can be found in Festa et al. (2011 a, b).

### *2.2 The TBM logged data*

The TBM Information System (here TBM-IS) logs all information concerning the TBM status and the construction process. This data can be grouped as: positioning, hydraulic pressures, fluids handling, status bits, currents, and voltages. Only hydraulic pressures, fluids handling, and status bits will be considered in this paper in order to describe the system of forces and pressures acting on the TBM. The positioning data were previously used to build the kinematic model described in Festa et al. (2011 a, b).

Data acquisition is a time-based continuous process. Each time step the signals from all the sensors are sequentially acquired and recorded. The time gap between two subsequent acquisitions varies between 5 and 6 seconds, and the data set is separated into individual files for each separate ring, with a new file created at the start of ring excavation. The shield advance is calculated based on the positioning data. However, the advance is not strictly increasing in time, since standstills, small shield fluctuations, and measurement accuracy can lead to a still, or even backward moving TBM. These aspects show up when discussing the data filtering process.

*2.3 Overview of forces*

Forces and pressures acting on the TBM can be subdivided in active and passive. The active ones include all actions subject to the control of the TBM operator (e.g. support pressure, advancing force, etc.). The passive include the reaction of the surrounding soil and fluids, and the interaction with the already installed concrete lining, i.e. all those actions which are not directly controllable. The distinction proposed reflects another substantial difference between the active and the passive group. While active forces and pressures can be derived from the TBM data set with limited processing, the passive ones can only be modelled. A list of all active and passive forces is given below, with further explanations in Figs. 1 and 2.

***Active components***:

$\boldsymbol{p_{cw-soil}}$: contact pressure between the cutting wheel and the soil;

$\boldsymbol{p_{sl}}$: hydrostatic pressure exerted by the face support fluid. This can be thought as acting on the bulkhead wall of the TBM;

$\boldsymbol{F_{cw}}$: cutting-wheel self-weight. It also includes the weights of the wheel support structure and of the main drive. Buoyancy effects of the immersed parts are accounted for;

$\boldsymbol{F_{sl}}$: weight of the support fluid filling the excavation chamber and (part of) the working one. Its value depends on the specific weight of the fluid and on the actual fluid level in the working chamber;

$\boldsymbol{F_{sw1}}$, $\boldsymbol{F_{sw2}}$, and $\boldsymbol{F_{sw3}}$: weights of the TBM-shield's front, central and rear part, respectively;

$\boldsymbol{F_{sw4}}$: self-weight of the concrete segment being handled by the erector before installation;

$\boldsymbol{F_{btr}}$: pulling-force due to the back-train;

$\boldsymbol{F_{thr}}$: longitudinal component of the advance force generated by the thrust cylinders.

***Passive components***:

$\boldsymbol{F_{bu}}$: buoyant force of the TBM-shield (ranging from the cutting-edge to the tail);

$\mathbf{T}_{\boldsymbol{thr}}$: shearing (transversal) component of the advance force generated by the thrust cylinders. This action can arise for at least two distinct reasons (or a combination of them). The first cause may be a transversal displacement between the TBM and the last installed ring. A displacement may be caused for example by a differential unit buoying force between the TBM-shield (or at least its rear part) and the final tunnel lining. The second reason may lie in a non-perfect alignment of the thrust cylinders (or some of them) with the shield longitudinal axis. Consequently, the thrust force is no more perpendicular to the plane where the cylinders are connected to the shield and a transversal component arises;

$\boldsymbol{F_{tb}}$ and $\boldsymbol{T_{tb}}$: normal and shear contact forces between the tail-brushes and the last-installed concrete ring. The tail brushes are designed to adhere to the final lining such as to prevent the inflow of the tail-void grout back into the TBM.

The adhesion is provided by their mechanical deformation and by the injection of pressurized grease between the rows of brushes. At Hubertus there were three rings of brushes installed, therefore with two rings of pressurized grease. If for some reason the final lining becomes eccentric with respect to the shield, an uneven distribution of the brushes deformations occurs and may originate a transversal component of force. Also an odd distribution of the friction between tail brushes and concrete lining may provoke the rise of a bending moment;

$p_{shl}$: contact pressure between the shield skin and the surrounding soil.

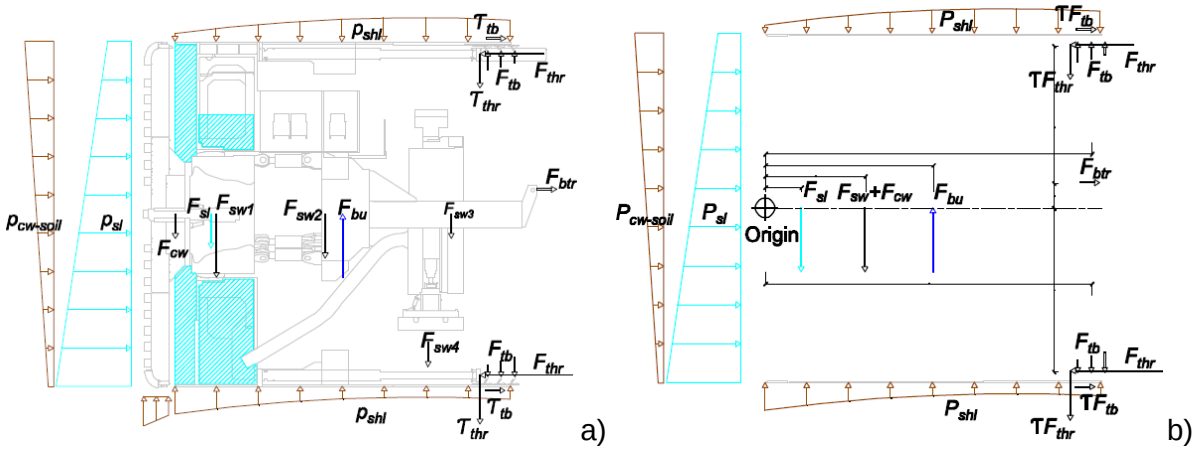


Figure 1 - Forces acting on the Hubertus Tunnel's TBM: schematic view, a); and calculation scheme, b)

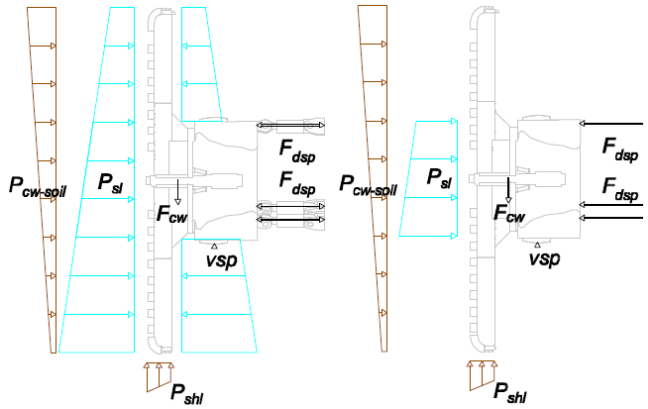


Figure 2 - Forces acting on the cutting wheel: decomposition of actions and use of internal forces

In Fig. 1 b), $\mathrm{Origin}$ indicates the reference point around which the balance of moments will be calculated. The arms of the forces with respect to $Origin$ are also indicated.

Conventionally, the forces are decomposed in vertical and horizontal components ($\boldsymbol{F_v}$ and $\boldsymbol{F_h}$), where $\boldsymbol{F_h}$ is assigned the same sign as $\boldsymbol{F_x}$ (see Fig. 3). The active forces may only be vertical (weights), or oriented parallel to the shield-axis. The moments are also decomposed in vertical and horizontal ($\boldsymbol{M_v}$ and $\boldsymbol{M_h}$). $\boldsymbol{M_{(rhr)}}$ is equivalent to the moment $\boldsymbol{M}$, according to the right-hand-rule. $\boldsymbol{M_h}$ is (by definition) horizontal, but also perpendicular to the shield-axis, which is a direct consequence of the (simplistic) assumption that the active forces are applied perpendicularly to the shield faces.

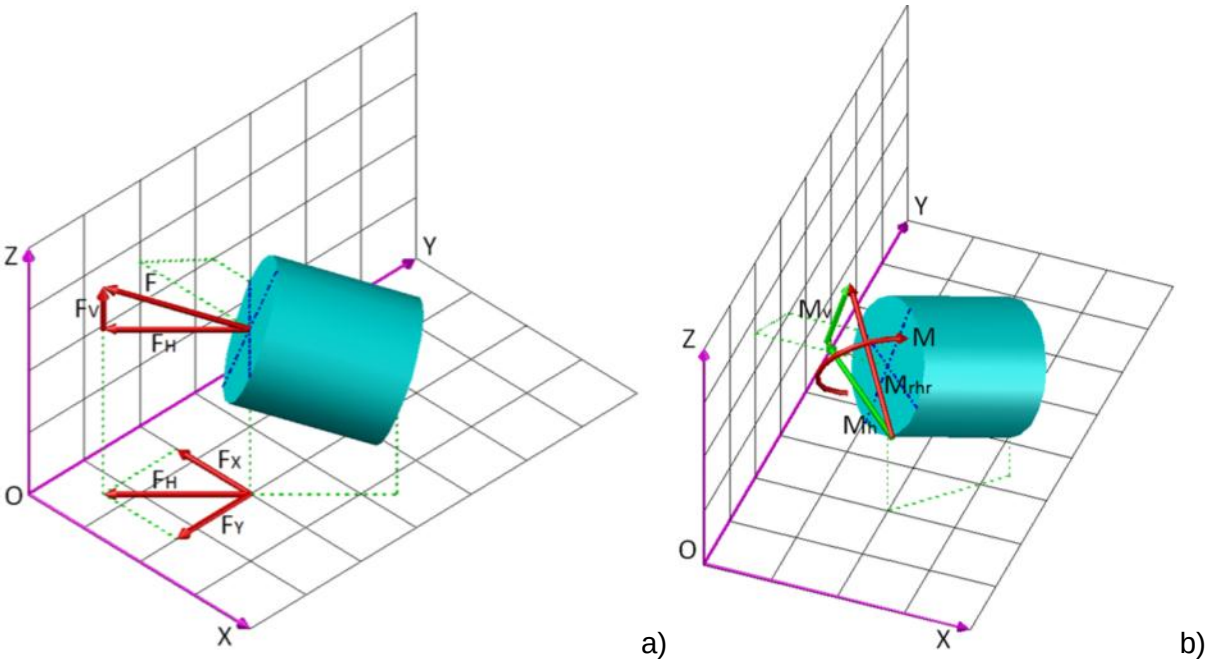


a) b)

Figure 3 – Sign convention for forces (a)) and moments (b)).

## 3 THRUST ACTION

The thrust-force was applied by 30 hydraulic cylinders, subdivided in 5 groups (A-E) formed by three pairs of cylinders each. The hydraulic pressure was the same for all the cylinders belonging to the same group. The (central) positions of the groups were: A at top; B at 72° (cw); C at 144° (cw); D and E symmetrical of C and B, with respect to the vertical axis. The total thrust force, plotted versus distance and time, is represented in Fig. 4 a). In Fig. 4 b), where the time-path of the thrust force is presented, the stepped release of the groups during ring construction is evident.

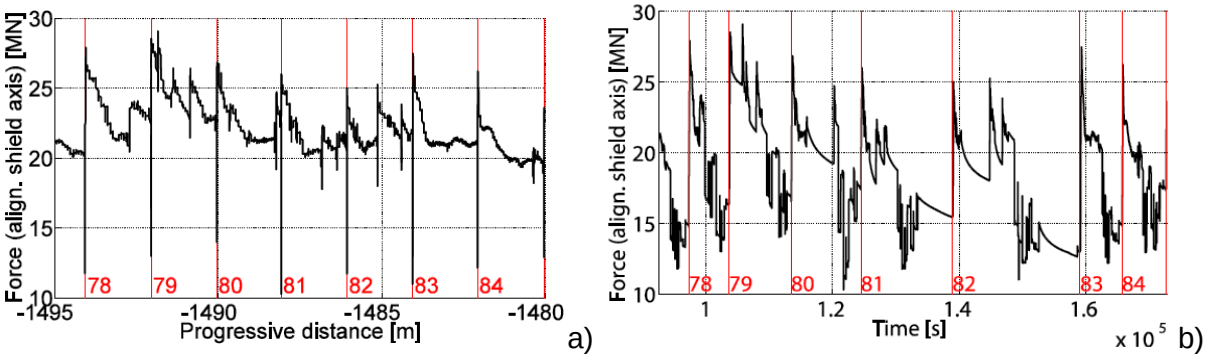


a) b)

Figure 4 – Total thrust force plotted versus distance (a)) and time(b)). In red ring numbers.

The moment applied by the thrust-cylinders is represented in Fig. 5 (vertical component) and Fig. 6 (horizontal component). A plot view with increased detail is provided in Fig. 7 and Fig. 8 a). The effects of the ring installation (segment by segment) are quite visible. Fig . 8 a) interestingly shows that at the end of the ring construction the horizontal applied turning moment is close to 5 MN, compared to the applied moment during drive which is around -40 MN. This is expected to influence the shield behaviour. Finally, in Fig. 8 b) the pull force on the TBM's back-trail is plotted. Given the low values registered, this can be disregarded.

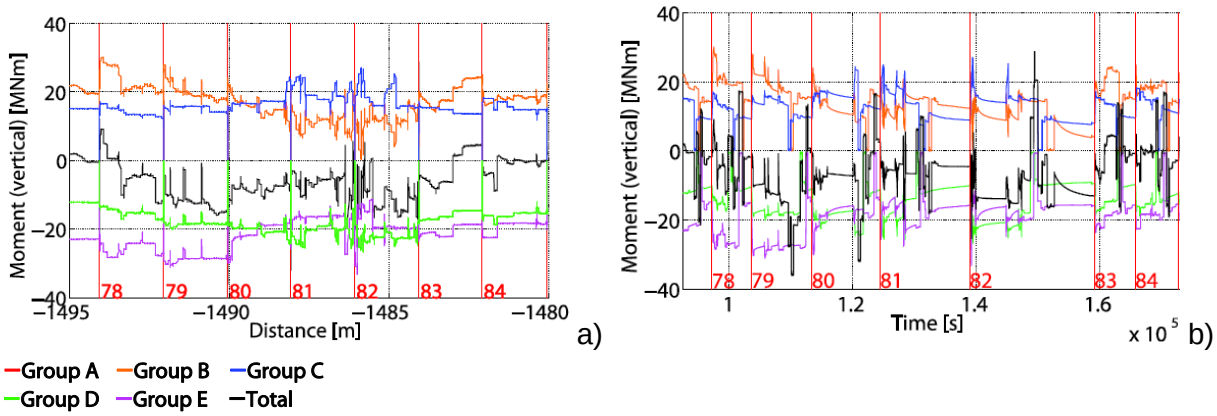


Figure 5 – Vertical moment due to the thrust groups and total value versus distance (a)) and time (b)). In red ring numbers.

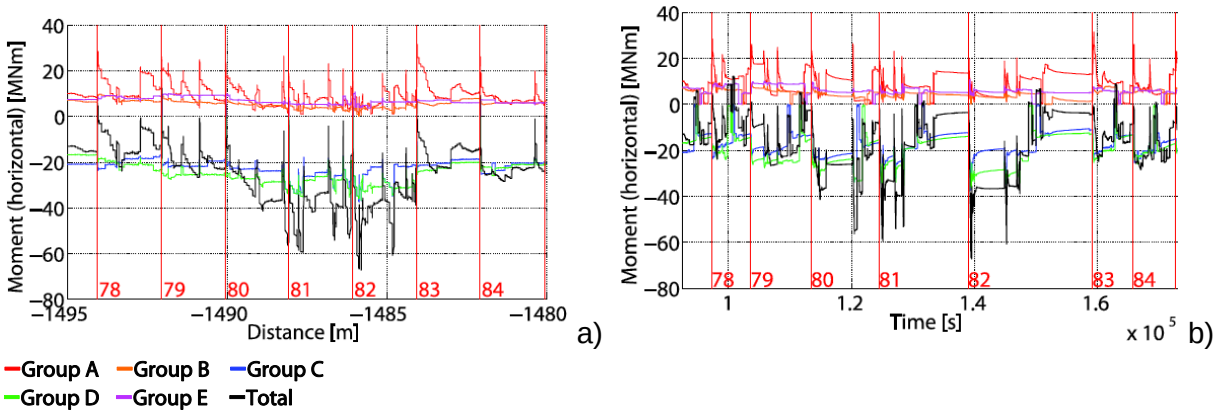


Figure 6 – Horizontal moment due to the thrust groups and total value versus distance (a)) and time (b)). In red ring numbers.

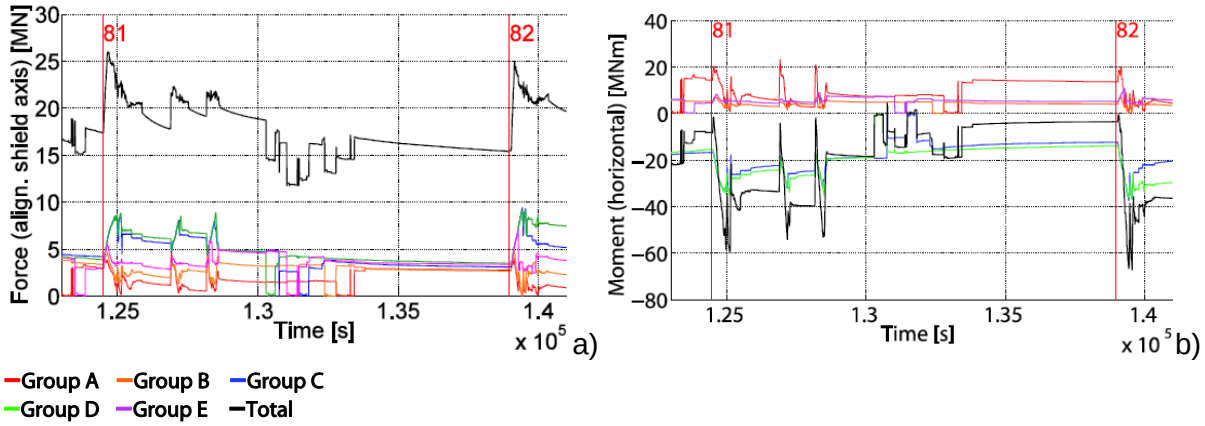


Figure 7 – Detail of the construction of ring 81 for thrust force (a)) and vertical moment (b)) versus time. In red ring numbers.

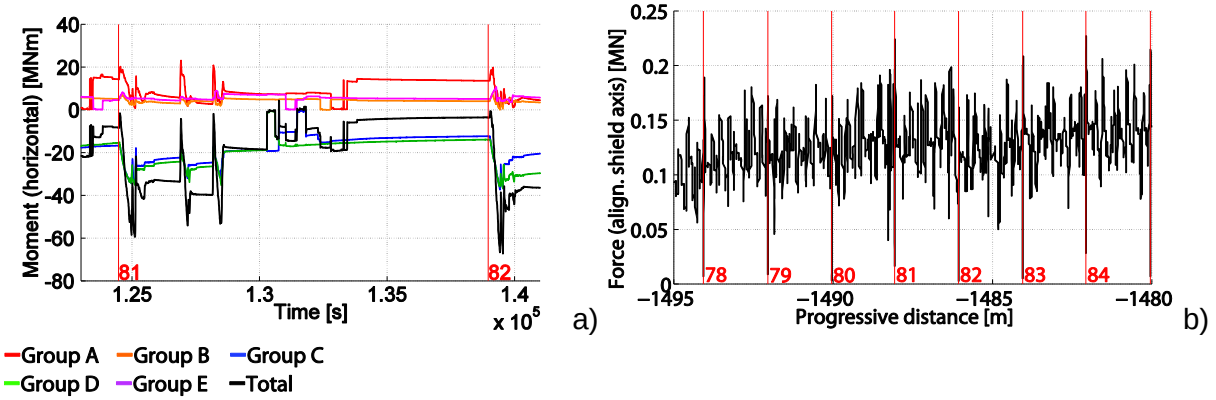


Figure 8 – Detail of the construction of ring 81 for horizontal moment versus time (a)). Pull force on the back-train (b)). In red ring numbers.

## 4 COMBINED RESULTS

In terms of horizontal components, the thrust force and the hydrostatic action of the excavation fluid were largely predominant over the other components. The horizontal resulting force ranged between -10 and -5 $\mathrm{MN}$ during driving, with a decreasing tendency (in absolute value) during each interval. During standstills for ring erection, the resultant horizontal force usually dropped to 0 $\mathrm{MN}$, with excursions in the positive field. Sign-concordance between resulting force and hydrostatic action of the support fluid means that the shield is pushed backward.

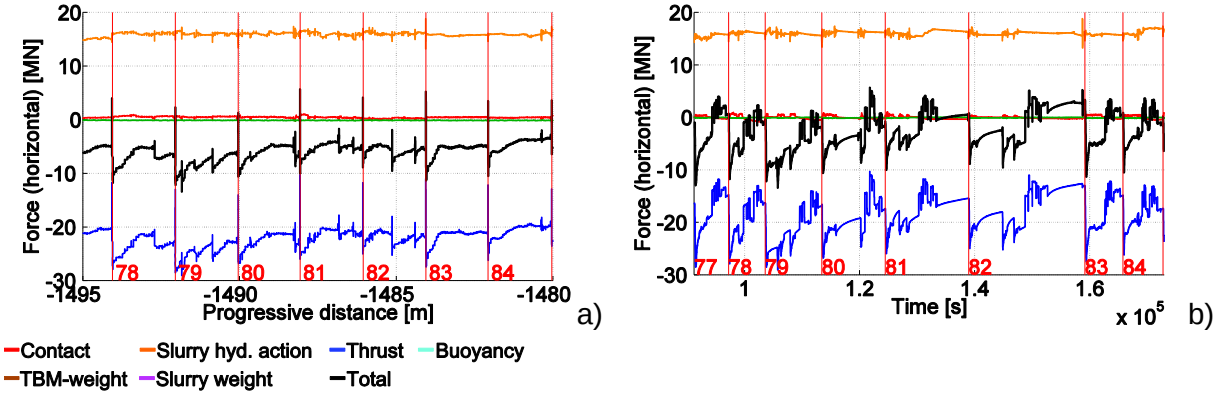


Figure 9 – Balance horizontal forces versus distance (a)) and time(b)). In red ring numbers.

The major actions in vertical direction are the TBM-weight, the uplift force due to buoyancy effect, and, at a lower order, the self-weight of the slurry in the excavation and working chambers. The effect of the other actions can be disregarded. The resulting (vertical) force fluctuated around 0 $\mathrm{MN}$, as shown in Fig. 10, suggesting that the vertical balance of the TBM is fully captured. Still, we have to consider that the buoyancy effect is a derived value calculated assuming a specific weight $\gamma_f = 10 \frac{\mathrm{kN}}{\mathrm{m}^3}$, and that a different specific weight would affect the equilibrium. For example, a specific weight of the fluid of $12 \frac{\mathrm{kN}}{\mathrm{m}^3}$ would provide a resultant uplift force of $1.8\ \mathrm{MN}$.

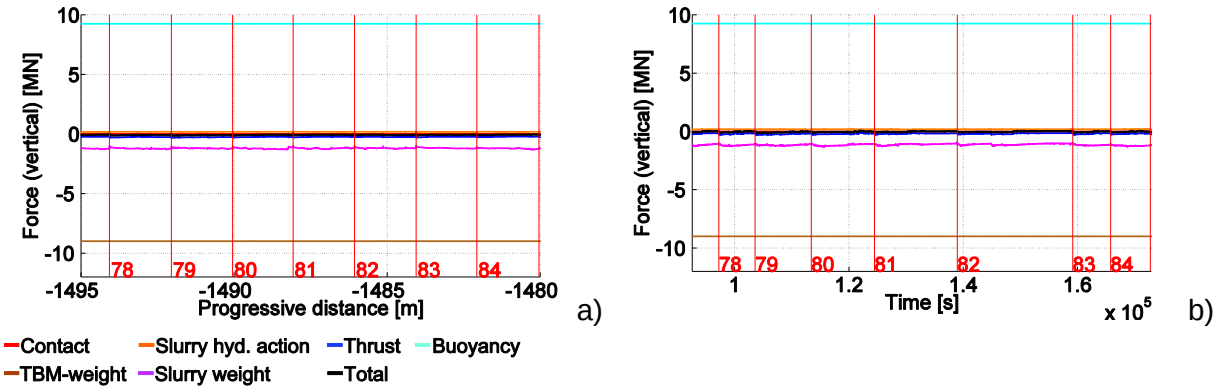


Figure 10 - Balance vertical forces versus distance (a)) and time(b)). In red ring numbers.

The contributions to the turning moment were relatively constant, except for the thrust actions. Consequently, the path of the resulting moment closely followed that of the thrust moment, apart from an offset of 24 MN for the horizontal component (Figs. 11 and 12). Two additional aspects may be mentioned. First, along the part of alignment investigated (from -1495 m to -1480 m), the resultant horizontal moment applied during drive ranged from +40 to -65 MN (see Fig. 11 b)). Second, even when concentrating on a single ring, the applied horizontal moment also significantly varied. For example, at ring 81 (Fig. 11 b)), the applied moment ranged from +30 to -35 MN. Similar observation can be made with reference to the vertical moments, as in Fig. 12. For this paper, a limited portion of the entire alignment of the two running tunnels was selected. However, data were processed and analysed along the entire extent of both tunnels.

The analysis of the TBM driving actions (pressures, forces, and moments), referred to as 'active forces', provided a comprehensive view on the actions applied. Nevertheless, since the active system remains unbalanced, an equilibrating system must exist. This 'passive system' is formed by the soil and process-fluids actions around the shield-skin (so called $\boldsymbol{P_{shl}}$), the radial and longitudinal actions due to the contact between tail-brushes and concrete lining ($\boldsymbol{F_{tb}}$ and $\boldsymbol{T_{tb}}$, respectively), and the transversal component of the thrust force ($\boldsymbol{T_{thr}}$). As the passive system was not monitored, these forces cannot be derived from direct data analysis, but must be modelled instead. The modelling is currently work in progress, and will be based on the results obtained from the kinematical analysis presented by Festa et al. (2011 a, b).

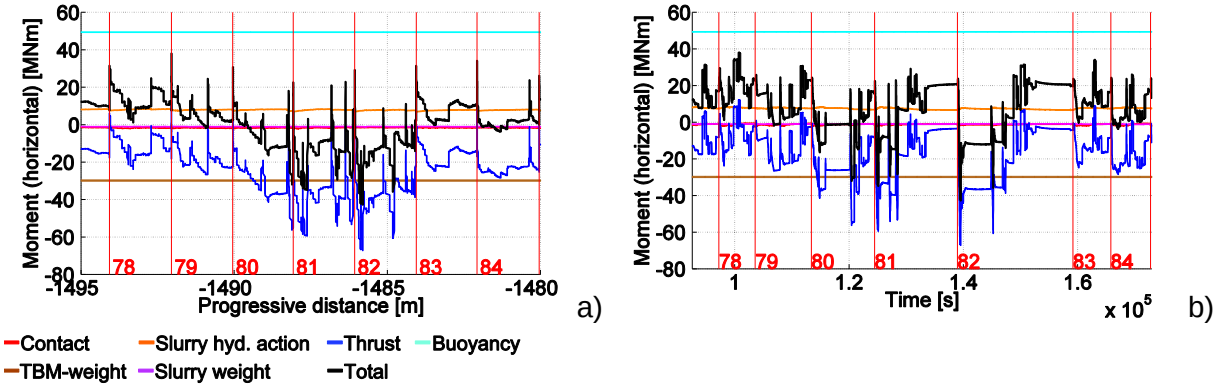


Figure 11 - Balance horizontal moment versus distance (a)) and time(b)). In red ring numbers.

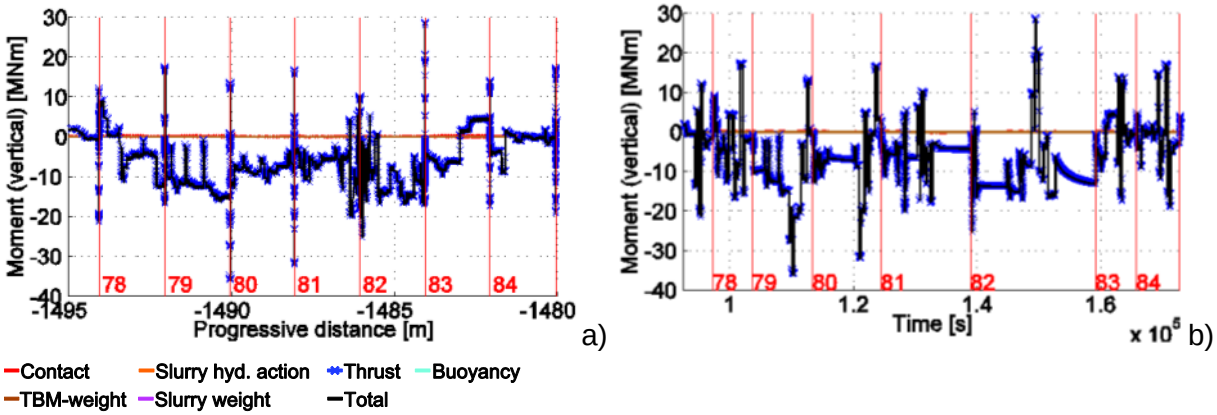


Figure 12 - Balance vertical moment versus distance (a)) and time(b)). In red ring numbers.

## 5 CONCLUSIONS

Pressure, forces, and turning moments applied to the slurry-shield Tunnel Boring Machine (TBM) used at the Hubertus Tunnel (The Hague, The Netherlands) have been obtained numerically by processing the logged machine operational data. The time and spatial resolution of the analysis were relatively high, since the time gap between subsequent registrations ranged from 5 to 10 seconds, and the corresponding advance varied from zero (during ring-erection standstills), to only few millimetres (during shield drive). Because of this accuracy, physical processes like the fluctuation in specific weight of the excavation fluid, and the thrust force's magnitude and spatial distribution have been visualized and discussed. Further, distance-based and time-based plots allowed for process-analysis during drive and during ring-erection, respectively.

The reconstruction of the applied driving actions is a partial contribution only to the full numerical modelling of the interactions between the TBM and the surrounding soil. Nevertheless, this study successfully quantified the 'missing link' to equilibrate the system of forces and turning moments. At this stage, modelling the external reaction acting on the TBM (i.e. surrounding soil, excavation fluids, and interaction with the already installed tunnel-lining) acting on the TBM might appear more problematic. Hopefully, at least part of this reaction, namely the stress distribution at the shield-soil interface, can be derived from observations on the kinematical interactions occurred and monitored while driving. This was the subject of previous publications, and is to undergo further developments. Finally, it has been shown that TBM's monitoring data, often relegated to a merely technological field, can promote advances in the fundamental engineering research field.

## REFERENCES

Kasper, T., Meschke, G., On the influence of face pressure, grouting pressure and TBM design in soft ground tunnelling, Tunnelling and Underground Space Technology, 21(2), 160-171 (2006)

Nagel, F.J. 2009. Numerical modelling of partially saturated soil and simulation of shield supported tunnel advance. PhD thesis report. Bochum: Institute for Structural Mechanics, Ruhr-University Bochum

Nagel, F., Stascheit, J., and Meschke, G., Process-oriented numerical simulation of shield tunneling in soft soils, Geomechanics and Tunnelling, 3(3), 268-282 (2010)

Festa, D. et al. 2011a. Tunnel-boring process in urban environment. Modelling for reliability: a kinematic study. Seventh International Symposium on Geotechnical aspects of underground construction in soft ground – 16-18 May 2011 – Rome – Italy

Festa, D. et al. 2011b. Tunnel-boring process in soft soils: improved modelling for reliability enhancement. Kinematic behaviour and tail grouting monitoring. ITA-AITES World Tunnel Congress – 20-26 May 2011 – Helsinki – Finland